Korean J. Chem. Eng., **29**(7), 876-885 (2012)
DOI: 10.1007/s11814-011-0263-6

Fabrication of electrolyte-impregnated cathode by dry casting method for molten carbonate fuel cells

Min Goo Kang*,*, Shin Ae Song*, Seong-Cheol Jang*,***, In-Hwan Oh*, Jonghee Han*,†, Sung Pil Yoon*, Sung-Hyun Kim**,†, and Seong-Geun Oh*****

*Fuel Cell Research Center, Korea Institute of Science and Technology, 39-1, Hawolgok-dong, Seongbuk-gu, Seoul 136-791, Korea
**Department of Chemical & Biological Engineering, Korea University, 1, Anam-dong, Seongbuk-gu, Seoul 136-701, Korea
***Major in Chemical Engineering, Hanyang University, 17, Haengdang-dong, Seongdong-gu, Seoul 133-791, Korea
(*Received 8 August 2011 • accepted 11 October 2011*)

Abstract−A dry casting method for fabricating a porous Ni plate, which was used as the cathode for molten carbonate fuel cells, was proposed, and the basic characteristics of the as-prepared cathode were examined and compared with those of a conventional cathode fabricated by using the tape casting method. Through several investigations, we confirmed that the cathode fabricated by using the dry casting method has properties identical to those of the conventional cathode. Electrolyte-impregnated cathodes were also successfully fabricated by using the dry casting method. Several characteristics of the as-prepared electrolyte-impregnated cathodes including their electrical performance were investigated by using tests such as the single cell test. The cell performances of a single cell using a 25-wt% electrolyte-impregnated cathode and not the electrolyte-impregnated cathode were 0.867 V and 0.819 V at a current density of 150 $mAcm^{-2}$ and 650 °C, respectively. The single cell using a 25-wt% electrolyte-impregnated cathode was also operated stably for 2,000 h. The cell performance was enhanced, and the internal resistance and the charge transfer resistance were reduced after electrolyte impregnation in the cathode. Moreover, the increase in the surface area of the cathode and the further lithiation of the NiO cathode after the electrolyte impregnation in the cathode enhance the area of the three-phase boundary and the electrical conductivity, respectively. However, the cell performance of the single cell using the 35-wt% electrolyte-impregnated cathode was reduced, and the cell could not be operated for a long time because of the rapid increase in the N_2 crossover caused by the poor formation of a wet seal.

Key words: Molten Carbonate Fuel Cell, Electrolyte-impregnated Cathode, Dry Casting Method

INTRODUCTION

Molten carbonate fuel cells (MCFCs) are high-temperature fuel cells that operate at around 923 K. The operation at high temperatures leads to high efficiency and produces high-quality waste heat; further, such operation makes it possible to use less expensive materials as cell components [1-8]. For many years, in-situ lithiated nickel oxide (NiO) has been commonly used as the cathode for MCFCs because of its stability in carbonate melts and an oxygen atmosphere and because of its high electrical conductivity [8-10]. In general, the Ni green sheet is first fabricated by using a conventional tape casting method; it is then sintered for the formation of a porous Ni plate at a high temperature under a reducing atmosphere. The cell is assembled using this prepared porous Ni plate as a cathode for the MCFCs. During the pre-treatment process in the cell, the electrochemical catalytic properties and the appropriate conductivity are realized through the in-situ oxidation and lithiation reactions of a porous Ni plate [9].

Tape casting is a well-known process used to produce a large-area, thin, and flat ceramic sheet that is difficult to fabricate using other methods such as pressing and extruding [11-16]. The largest advantage of tape casting is the good thickness control of the large-area and thin ceramic sheet [12]. A slurry consisting of the ceramic powder, dispersants, binders, and plasticizers in organic solvents is casted onto a stationary or moving surface for the fabrication of a ceramic sheet [13]; the detailed procedure for the tape casting is illustrated in Fig. 1(a). However, the tape casting method is a complex and long process that includes the preparation of the slurry for making a green sheet, deaeration, tape casting, and drying of organic solvents. As the solvent-based tape casting technology always involves the use of toxic solvents and hazardous additives, it increases the production cost and poses considerable harm to human health and the environment [14]. In this study, to solve these problems, we developed a new fabrication method for the MCFC electrode, and named this method the "dry casting method." The procedure of the dry casting method is shown in Fig. 1(b). As shown in Fig. 1(b), the dry casting method is a very simple process and does not use any organic materials such as toxic solvents and hazardous additives. Hence, it is eco-friendly. Further, the production cost can be reduced through a process simplification by eliminating processes such as the preparation of the slurry required for fabricating a green sheet, deaeration, and drying of organic solvents.

One of the main issues related to the MCFC stack is the retention of electrolyte in the components to prevent a decrease in the height of the stack caused by the melting of the electrolyte sheets between

†To whom correspondence should be addressed.
E-mail: jhan@kist.re.kr, kimsh@korea.ac.kr

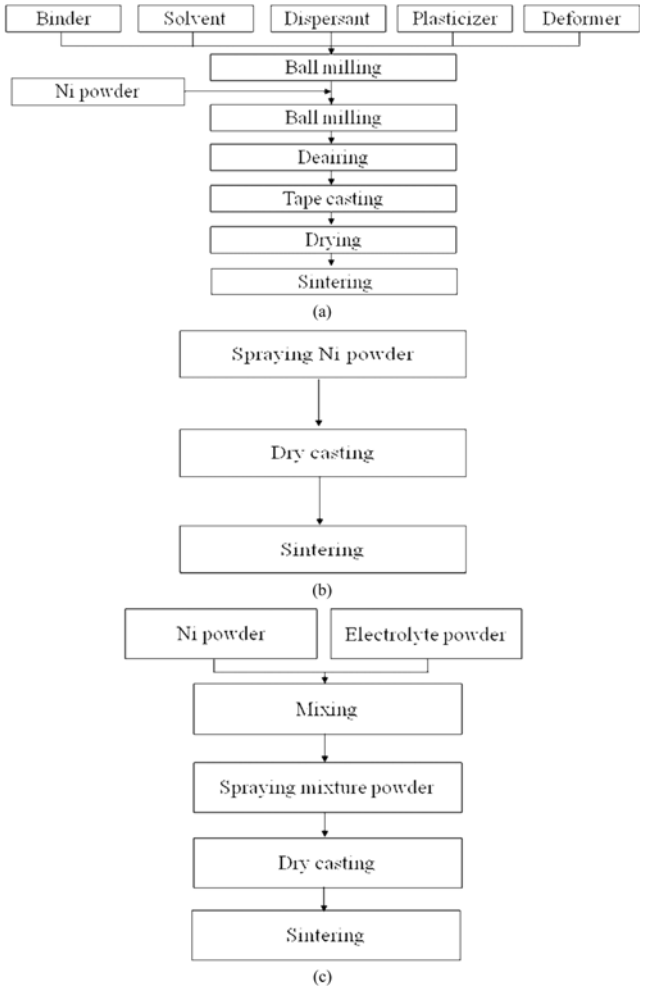

Fig. 1. Fabrication of MCFC electrode: (a) conventional tape casting method, (b) proposed dry casting method, and (c) modified dry casting method for fabricating electrolyte-impregnated cathode for MCFC.

the matrix sheets during the pre-treatment process before the MCFC stack operation. The decrease in the stack height exerts continuous stress on the MCFC stack because the joint between the MCFC stack and the exterior manifold that supplies the reactant gases is not fitted as the height of the stack may decrease because of the melting of the electrolyte. This continuously exerted stress inhibits the long-term operation of the MCFC stack, which is required to have a 40,000-h operation to be commercially viable. The melting of the electrolyte sheets between the matrices during the pretreatment period induces the irregular distribution of the plate pressure and the initial electrolyte loss [17] and degrades the cell performance. To solve these problems, a few researchers developed a method for impregnating the electrolyte into an MCFC component such as the cathode, anode, or matrix [17-19]. However, there are few reports on the effect of electrolyte impregnation in the MCFC component.

In this study, we fabricated the MCFC cathode by using the proposed dry casting method and investigated the basic characteristics of the prepared cathode, such as pore size distribution, porosity, and electrochemical performance, by performing a single cell test. These characteristics of the MCFC cathode were compared with those of a conventional cathode fabricated by using a tape casting method. The electrolyte-impregnated cathode was also prepared by using the proposed dry casting method. The influences of the electrolyte impregnation into the cathode on the porosity, pore size distribution, and electrochemical performance of the cathode were investigated.

EXPERIMENTAL

1. Fabrication of NiO Cathode

The porous Ni plate that acts as an in-situ lithiated NiO cathode in the cell during the pretreatment process was fabricated by the dry casting method using Ni powder (INCO Co., Ltd.). For suppressing the formation of lumps when the Ni powder is filled in the mold, the Ni powder was dried at 120 °C for 24 h before the filling process. The dried Ni powder was spread in the stainless steel mold (thickness: 0.08 cm, size: 18 cm×18 cm) on the graphite plate. The spread Ni powder was filled evenly with a uniform thickness in the mold by using another graphite plate that was slid horizontally and slowly on the Ni powder: the "dry casting method." Then, the Ni powder in the stainless steel mold on the graphite plate was heat-treated at 800 °C for 3 h under a reducing atmosphere ($N_2 : H_2$= 90 : 10) for the formation of a Ni plate.

2. Fabrication of Electrolyte-impregnated Cathode

An electrolyte-impregnated cathode was also fabricated by using the dry casting method. The electrolyte composed of Li_2/K_2CO_3 (molar ratio=62 : 38, Daejung Chemicals and Metals Co. Ltd.) and Ni powder (INCO Co., Ltd.) was used for fabricating the electrolyte-impregnated cathode. The Ni powder and the electrolyte powder were mixed using a ball mill for 24 h. Before mixing, the Ni and electrolyte powders were dried completely at 120 °C for 24 h because of the highly hygroscopic nature of the electrolyte. The electrolyte was mixed with the Ni powder in amounts of 25 wt%, 35 wt%, and 45 wt%. The as-prepared mixed powder was spread in the stainless steel mold on the graphite plate. As mentioned earlier, the mixed powder was also filled in the mold evenly by using a method identical to the dry casting method. The filled mixed powder was also heat-treated at 580 °C for 3 h under a reducing atmosphere ($N_2 : H_2$=90 : 10) for the fabrication of the impregnated cathode.

3. Characterization of Cathode

The particle sizes of the Ni and the electrolyte powders were evaluated by a particle size analyzer (Horiba LA-300). Before and after the single cell test, the characteristics of the cathodes prepared by using the dry casting method were analyzed by the following methods. The porosity was measured by using the Archimedes method (ASTM C373-88), and the pore size distribution and the median pore diameter (MPD) were examined by the mercury porosimeter (Micrometrics Autopore II) analysis. The structures of cathodes prepared by using the dry casting method after cell operation were examined by X-ray diffraction (XRD, Rigaku RINT-2500) using Cu$K\alpha$ radiation. The morphologies of cathodes prepared by using the dry casting method before and after cell operation were examined by environmental scanning electron microscopy (ESEM, Gatan FEI XL-30 FEG) to observe the microstructure of the electrode.

4. Single Cell Test

The single cells having pure Ni and electrolyte-impregnated cathodes fabricated by using the dry casting method had an effective

Table 1. Operating conditions of single cells

Unit cell components	Values
Anode electrode and current collector	
Size (width×length, cm×cm)	11×11
Materials (electrode; current collector)	Ni-5-wt%Al; Ni
Mole ratio of fuel gas (H_2 : CO_2 : H_2O)	72 : 18 : 10
Total flow rate	365 cc min^{-1}
Cathode electrode and current collector	
Size (width×length, cm×cm)	10×10
Materials (electrode; current collector)	X-wt%E-DC cathode, DC cathode and TC cathode; SUS316
Mole ratio of fuel gas (air : CO_2)	70 : 30
Total flow rate	950 cc min^{-1}
Electrolyte	
Li_2CO_3/K_2CO_3 mole ratio	62 : 38
Matrix	α-$LiAlO_2$

area of 100 cm^2 and were operated at 650 °C to evaluate the performance of the as-prepared cathodes. In all the single cells, the anode of the Ni-5-wt%Al alloy, α-$LiAlO_2$ matrix, and the Li_2/K_2CO_3 electrolyte sheet prepared by using the tape casting method were used identically. The detailed operational conditions of the single cells are listed in Table 1. Under the standard operating conditions, a mixture of air and CO_2 was used as the cathode gas, and a mixture of H_2, H_2O, and CO_2 was used as the fuel gas. The flow rate of the reaction gas was fixed at 0.4 for the fuel and air utilization of H_2 and CO_2 in the anode and cathode gases. The H_2O in the anode gas was supplied using a water bubbler set to 50 °C. The cell performance was evaluated by measuring the cell voltage at various current densities. A DC current was applied to the cell using an electric loader (ELTO DC Electronics Co., ESL300Z). To analyze the electrode polarization, an electrochemical impedance analysis (EIS) was carried out in the open circuit condition (OCV) using Solartron S11287 and 1255B. The frequency range of the present EIS experiment was from 10,000 to 0.01 Hz. To measure the N_2 crossover, the gas composition of the anode outlet gas was measured by gas chromatography (GC, Hewlett-Packard 5890 series II).

RESULTS AND DISCUSSION

1. Non-electrolyte-impregnated Cathode

The basic characteristics of a pure Ni plate fabricated by using the dry casting method (DC cathode), such as SEM, pore size distribution, MPD, porosity, and plate thickness, were measured and compared with those of a conventional pure Ni plate fabricated by using the tape casting method (TC cathode, Twin Energy Co., Ltd., South Korea). Fig. 2 shows the SEM images of the DC cathode and the TC cathode. A typical morphology having a branched structure was observed in both samples. The branches were formed by the neck growth in the Ni powder after the heat treatment of both samples. The microstructure of the DC cathode was considerably analogous to that of the TC cathode.

It is generally well known that the optimal MPD and the porosity of a porous Ni plate used as an MCFC cathode are 8-10 μm and 70-80%, respectively [20]. The pore size distributions of the DC

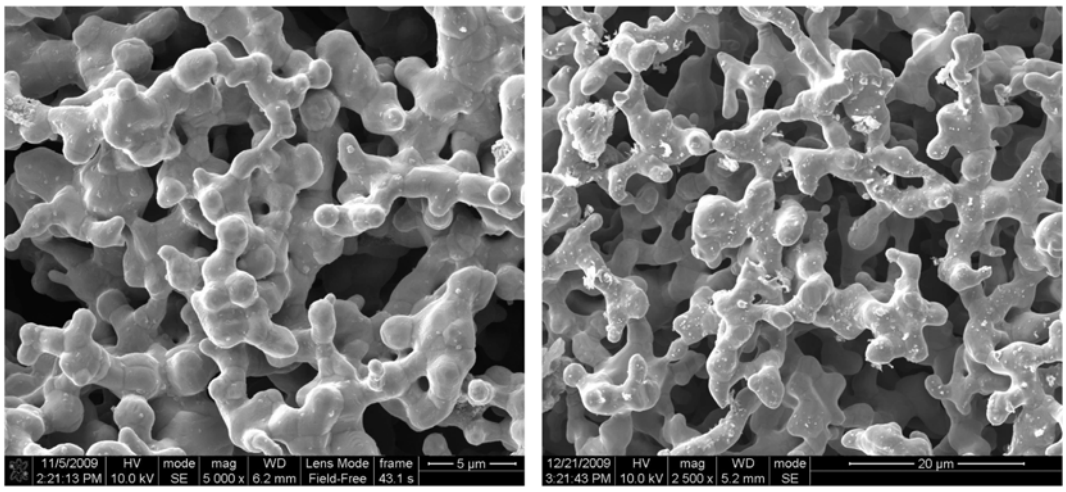

Fig. 2. SEM images of (a) TC cathode and (b) DC cathode.

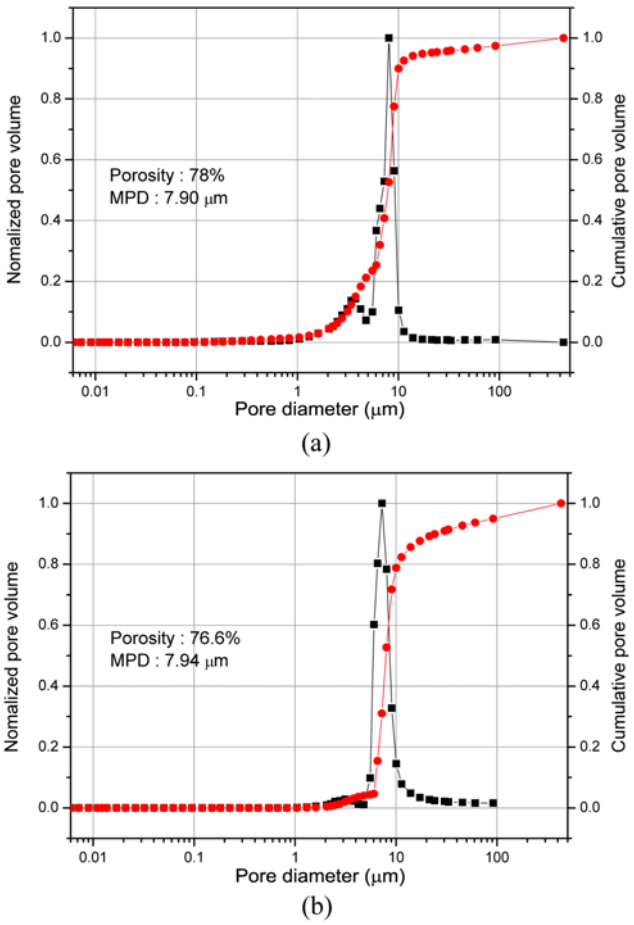

Fig. 3. Pore size distributions of (a) TC cathode and (b) DC cathode.

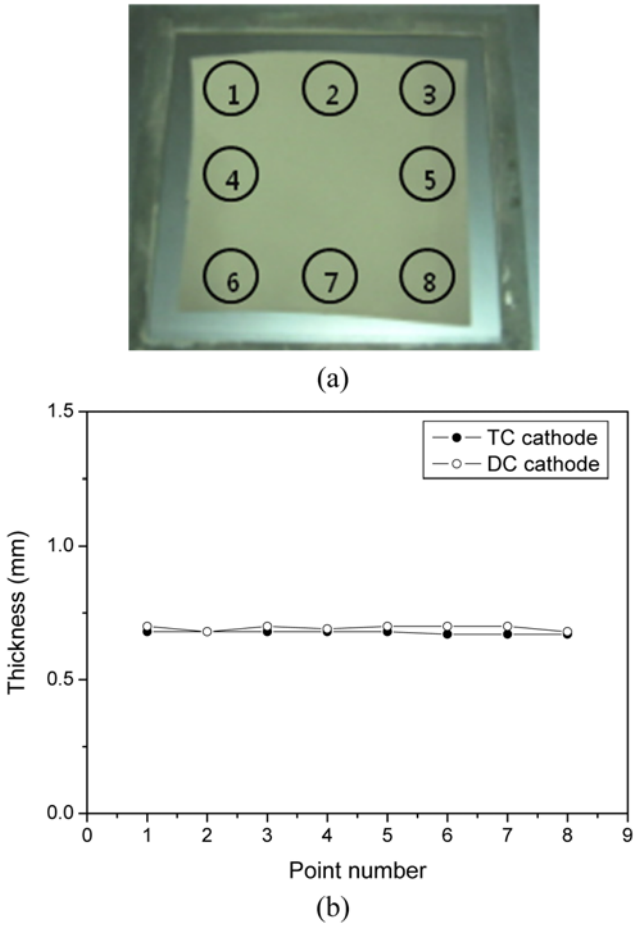

Fig. 4. Thickness deviations of cathodes: (a) picture of DC cathode and (b) graph of thickness deviation in TC cathode and DC cathode.

cathode and the TC cathode are shown in Fig. 3. As shown in Fig. 3, the pore size distributions of the DC cathode and the TC cathode were very similar; these cathodes also had a similar MPD of 7.94 μm and 7.90 μm, respectively. These MPD values of the two cathodes were included in the above-mentioned optimal MPD range of an MCFC cathode. The porosities of the two cathodes were also compared. The porosities of the DC cathode and the TC cathode were 76.6% and 78.0%, respectively. These porosity values were also within the optimal range of an MCFC cathode. From the results of a comparison of the basic characteristics of the two cathodes, we could confirm that the cathode fabricated by using a very simple dry casting method had characteristics identical to those of a conventional cathode fabricated by using the tape casting method.

To examine the thickness uniformity of the two cathodes, the thicknesses at eight points of the DC cathode and the TC cathode (size: 10 cm×10 cm) were measured. The poor thickness uniformity of an electrode exerts stress on the component materials inside the cell and induces some cracks or transformation in the component materials because of the degraded cell performance and poor stability. In general, to obtain uniform thickness, the tape casting method was used for fabricating the electrode. As shown in Fig. 4, we could confirm that the DC cathode had thickness uniformity similar to that of the TC cathode. As apparent from the comparison of the basic characteristics of the DC cathode and the TC cathode, the dry casting method is an extremely attractive candidate method for the fabrication of an MCFC electrode.

To examine the electrochemical performance of the DC cathode and to compare it with that of the TC cathode, we performed the single cell test. The results of the operation of single cells using the TC cathode and the DC cathode are presented in Fig. 5. The performances of the single cells at current densities of 50, 100, and 150 $mAcm^{-2}$ were evaluated at 650 °C in a standard gas composition of $U_f=U_o=0.4$. The internal resistance (IR, mΩ), which is the ohmic resistance (Ωcm^2) divided by the cell area (cm^2), and the N_2 crossover (%) are also checked to better understand the cell operation. As shown in Figs. 5(a) and 5(b), the performances of single cells using the TC cathode and the DC cathode at a current density of 150 $mAcm^{-2}$ were 0.810 V and 0.819 V, respectively. The similar performances of the single cells using the two cathodes are shown because the two cathodes have similar basic characteristics. In the two single cells, the cell performance gradually decreased with an increase in the IR and the N_2 crossover after a 400-h operation in the case of the single cell using the TC cathode and after a 700-h operation in the case of the single cell using the DC cathode. This could be attributed to the formation of voids in the matrix because of an electrolyte shortage.

2. Electrolyte-impregnated Cathode

The electrolyte-impregnated cathode (X-wt%E-DC cathode) was

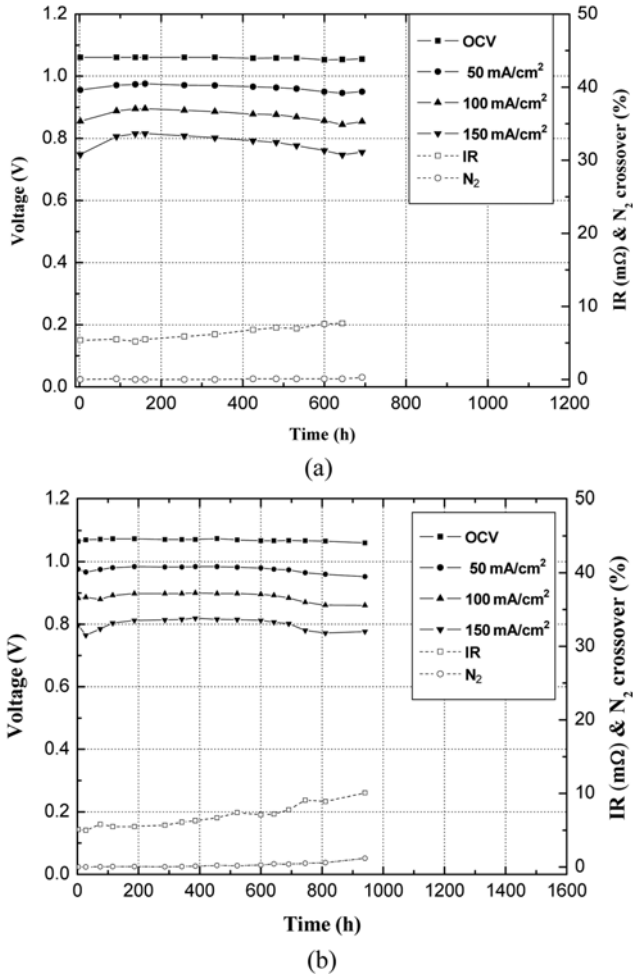

Fig. 5. Operating results of single cells using (a) TC cathode and (b) DC cathode.

fabricated by using a method similar to the proposed dry casting method. The particle sizes of the Ni powder and the electrolyte powder used for fabricating the electrolyte-impregnated cathode were 4.5 μm and 0.58 μm, respectively. The amount of electrolyte used was varied at different ratios of 25 wt%, 35 wt% and 45 wt%, and each mixture was prepared by mixing the Ni and the electrolyte powders with a ball mill for 24 h. The mixture of the Ni and X-wt% electrolyte powders was filled in the mold and sintered at 580 °C for 3 h under a reducing atmosphere for the formation of a porous electrolyte-impregnated cathode. The basic characteristics of the X-wt%E-DC cathodes fabricated by using the dry casting method, such as porosity, pore size distribution, MPD, and SEM, were measured and compared with those of the DC cathode. First, the porosities of the as-prepared X-wt%E-DC cathodes were investigated by using the Archimedes method (ASTM C373-88). Before measuring the porosity, we removed the electrolyte impregnated in the as-prepared X-wt%E-DC cathodes by immersing and boiling the cathodes in water for 2 days. The porosities of the 25-wt%E-DC cathode, 35-wt%E-DC cathode, and 45-wt%E-DC cathode after the electrolyte extraction were 72.3%, 78.2%, and 80.8%, respectively. The porosities of the X-wt%E-DC cathodes increased a little with an increase in the electrolyte content. However, all porosity values of

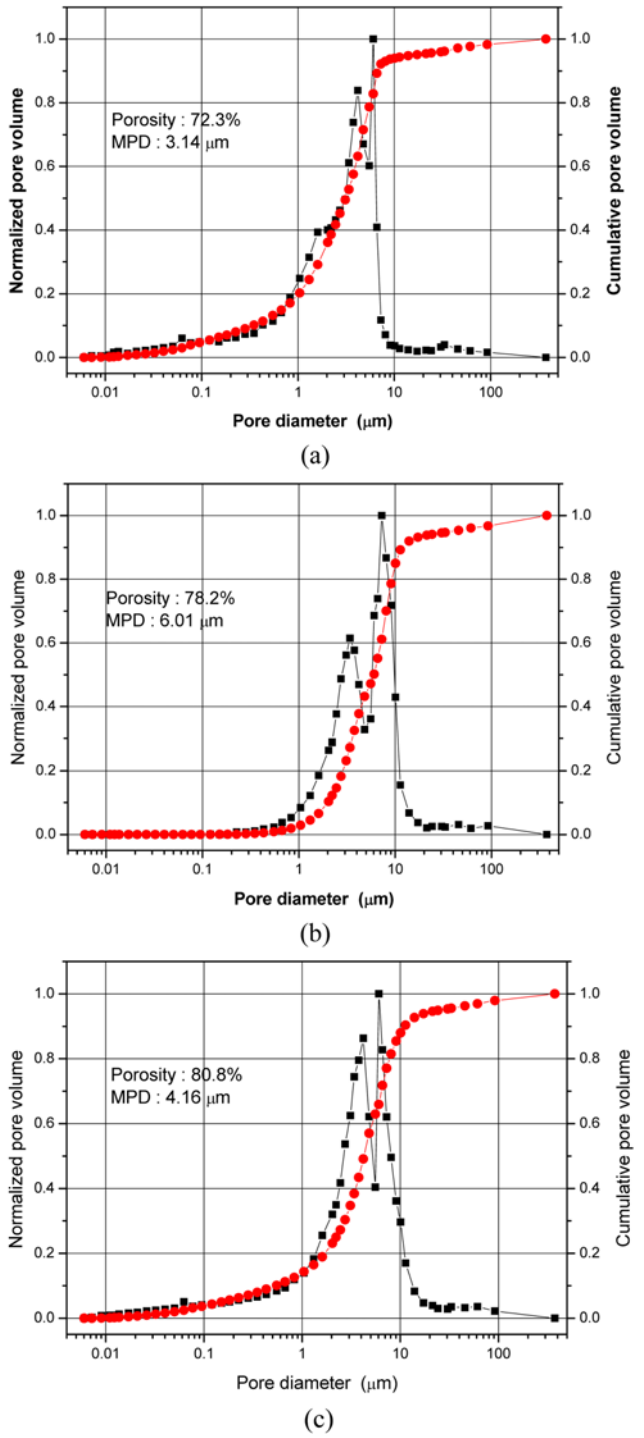

Fig. 6. Pore size distributions of (a) 25-wt%E-DC cathode, (b) 35-wt%E-DC cathode, and (c) 45-wt%E-DC cathode after electrolyte extraction.

the X-wt%E-DC cathode were within the range of optimum porosity.

The pore size distributions of the X-wt%E-DC cathodes are presented in Fig. 6. As shown in Fig. 6, the double pore structures having small pores and large pores were observed in the electrolyte-impregnated cathode, and the tendency of the double pore structures became clearer with an increase in the amounts of the impregnated electrolyte. The small pores in the electrolyte-impregnated cathode

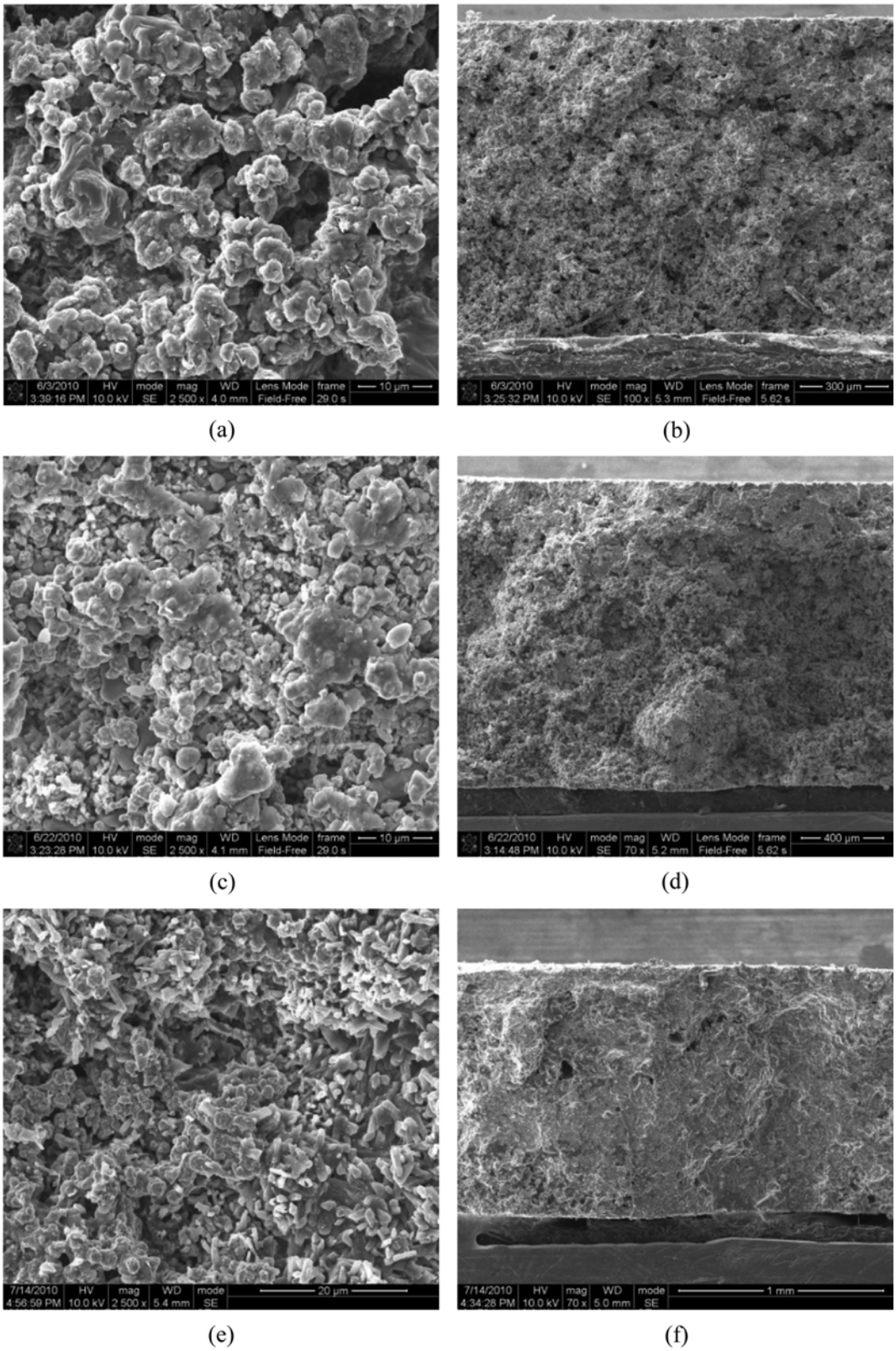

Fig. 7. SEM images of X-wt%E-DC cathodes before electrolyte extraction: (a) surface image of 25-wt%E-DC cathode, (b) cross-sectional image of 25-wt%E-DC cathode, (c) surface image of 35-wt%E-DC cathode, (d) cross-sectional image of 35-wt%E-DC cathode, (e) surface image of 45-wt%E-DC cathode, and (f) cross-sectional image of 45-wt%E-DC cathode.

might be formed from the impregnated electrolyte after the electrolyte extraction because of the use of an electrolyte powder finer than the Ni powder in the fabrication of the electrolyte-impregnated cathode.

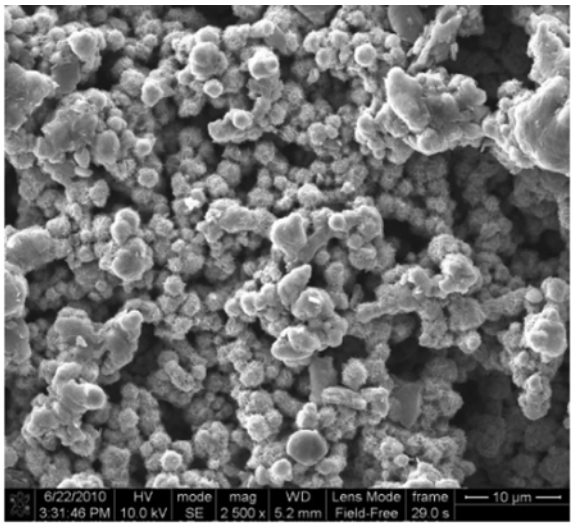

(a)

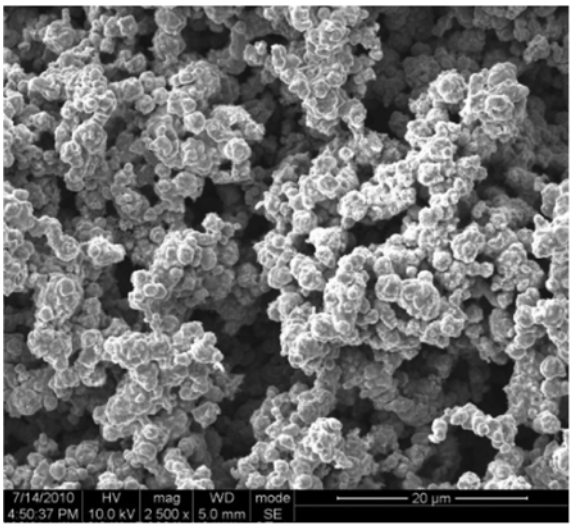

(b)

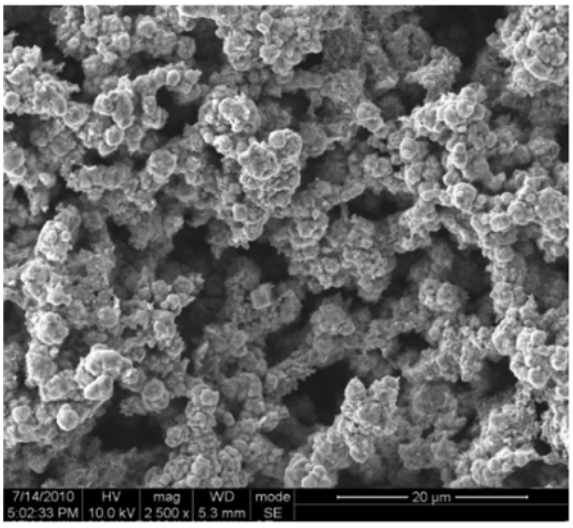

(c)

Fig. 8. SEM images of X-wt%E-DC cathodes after electrolyte extraction: (a) 25-wt%E-DC cathode, (b) 35-wt%E-DC cathode, and (c) 45-wt%E-DC cathode.

The SEM images of the X-wt%E-DC cathodes before and after the electrolyte extraction are shown in Figs. 7 and 8, respectively. First, as shown in Figs. 7(b), (d), and (f), the large pores disappeared with an increase in the amounts of the impregnated electrolyte, and few pores were even observed in the 45-wt%E-DC cathode. All these pore spaces were occupied by the electrolyte when the amount of electrolyte in the mixture was increased. The same tendency was observed in the top-view SEM images. In the top-view SEM image of the 25-wt%E-DC cathode, a few pores were observed, whereas no pores were observed in the top-view SEM images of the 35- and 45-wt%E-DC cathodes. As shown in Fig. 8, the necking morphologies among the Ni particles were not observed in any of the X-wt%E-DC cathodes after the electrolyte extraction, whereas the DC cathode (not electrolyte-impregnated cathode) fabricated by using the dry casting method had a necking structure sintered among the Ni particles (refer to Fig. 2(b)). The reason why the X-wt%E-DC cathodes did not have the branched structure was the heat treatment carried out at a low temperature for the fabrication of the electrode. The X-wt%E-DC cathodes were heat-treated at 580 °C for 3 h, whereas the DC cathode was heat-treated at 800 °C for 3 h. The reason why the X-wt%E-DC cathodes were heat-treated at a relatively low temperature was the low melting point of the electrolyte. The melting point of the eutectic melts was well known to

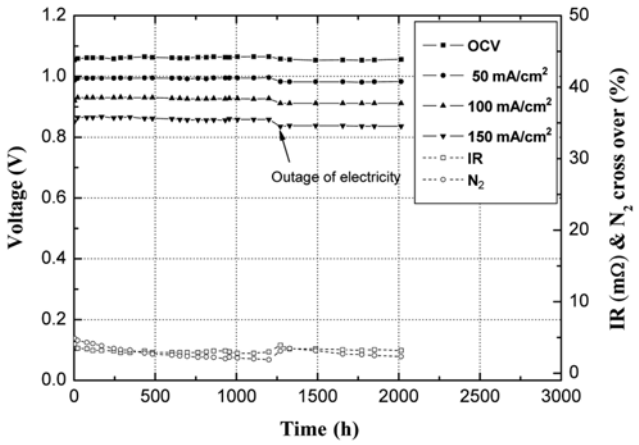

(a)

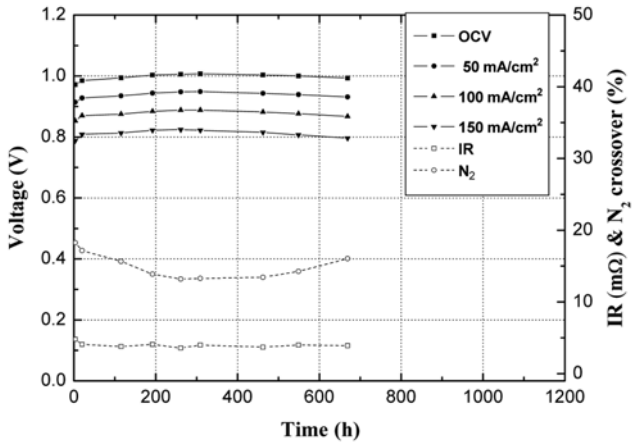

(b)

Fig. 9. Operating results of single cells using (a) 25-wt%E-DC cathode and (b) 35-wt%E-DC cathode.

Table 2. Comparisons of single cell operation with X-wt%E-DC cathodes

Amount of electrolyte	OCV (V)	Performance (V) at 150 $mAcm^{-2}$	IR (mΩ)	N_2 crossover (%)
0 wt%	1.071	0.819	5.1	0.1
25 wt%	1.061	0.867	3.2	2.3
35 wt%	1.006	0.824	3.2	13.2

be around 480 °C [21]. The fabrication of the electrolyte-impregnated cathode at a higher temperature or for a longer duration than the aforementioned condition of the heat treatment resulted in the electrolyte distribution in the cathode to lean toward the bottom of the cathode because the eutectic melts flowed downward. At the end of several trial and errors, the conditions of the heat-treatment fabrication of the impregnated cathode were fixed at 580 °C for 3 h.

To examine the electrochemical performance of the X-wt%E-DC cathodes, the single cell tests using the DC cathode, 25-wt%E-DC cathode, and 35-wt%E-DC cathode were carried out at 650 °C and a standard gas composition of $U_f=U_o=0.4$. The operating results of single cells using the 25-wt%E-DC cathode and the 35-wt%E-DC cathode are presented in Fig. 9. The operating results of the single cell using the DC cathode are already shown in Fig. 5(b). To compare the operating results of the three cells, the cell performance at a current density of 150 $mAcm^{-2}$, IR, and N_2 crossover in the three single cells using the DC cathode, 25-wt%E-DC cathode, and 35-wt%E-DC cathode are summarized in Table 2. As shown in Table 2, the cell performances of single cells using the DC cathode, 25-wt%E-DC cathode, and 35-wt%E-DC cathode at a current density of 150 $mAcm^{-2}$ were 0.819, 0.867, and 0.824 V, respectively. Further, the IR values of single cells using the DC cathode, 25-wt%E-DC cathode, and 35-wt%E-DC cathode were 5.1, 3.2, and 3.2 mΩ, respectively. The cell performance increased and the IR decreased after the electrolyte impregnation in the cathode. When the amount of the impregnated electrolyte in the cathode was 25 wt%, the cell performance was the highest and the IR was the lowest in our experiments. As shown in Table 3, the surface areas of the DC cathode, 25-wt%E-DC cathode, 35-wt%E-DC cathode, and 45-wt%E-DC cathode before the cell operation were 0.26, 2.32, 2.54, and 3.32 m^2g^{-1}, respectively, and the surface areas of the DC cathode, 25-wt%E-DC cathode, and 35-wt%E-DC cathode after the cell operation were 0.48, 0.69, and 0.93 m^2g^{-1}, respectively. After the electrolyte impregnation, the surface areas increased dramatically. The large decrease in IR in the single cells after the electrolyte impregnation was brought about by the increase in the contact area between the eutectics melts and the Ni surface of the electrode in the cells.

Table 3. Surface areas of DC cathode and X-wt%E-DC cathodes before and after cell operation

Cathode	Surface areas before cell operation (m^2g^{-1})	Surface areas after cell operation (m^2g^{-1})
DC cathode	0.26	0.48
25-wt%E-DC cathode	2.32	0.69
35-wt%E-DC cathode	2.54	0.93
45-wt%E-DC cathode	3.32	-

However, the cell performance of the single cell using the 35-wt%E-DC cathode that has a larger surface area than and an IR value similar to those of the 25-wt%E-DC cathode was lower than that of the 25-wt%E-DC cathode. This result was attributed mainly to the rapid increase in the reactant gas crossover. As shown in Fig. 9(b) and Table 2, the N_2 crossover in the single cell using the 35-wt%E-DC cathode increased dramatically as compared that of the DC cathode and the 25-wt%E-DC cathode. The main cause of this rapid increase in the N_2 crossover in the cell using the 35-wt%E-DC cathode was confirmed to be the poor formation of the wet seal after the cell disassembly. The wet seal at the edge of the cell frames was not formed well in the single cell using the highly electrolyte-impregnated cathode because the electrolyte amount added among the matrices was reduced for the addition of the same amount of electrolyte in each single cell during the assembly of the single cells using the DC cathode and the X-wt%E-DC cathodes. This poor wet seal promoted the air entrance into the cell interior during the cell operation. However, the single cell using the 25-wt%E-DC cathode was operated considerably stably although the N_2 crossover was more than 2%, which is a significantly high value. In the case of the 35-wt%E-DC cathode, however, it was difficult to operate the single cell for more than 700 h because of the extremely high N_2 crossover. After the cell disassembly, it was confirmed that the anode became black due to oxidation by the entered air via the poor wet seal.

The Nyquist plots of the single cells using the DC cathode, 25-wt%E-DC cathode, and 35-wt%E-DC cathode are presented in Fig. 10. The Nyquist plots show two arcs and one intercept on the x-axis for every single cell; these shapes are typically obtained in the

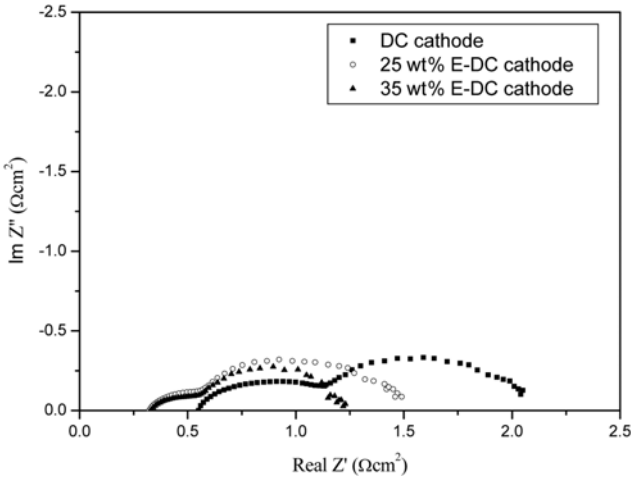

Fig. 10. Nyquist plots of single cells using DC cathode, 25-wt%E-DC cathode, and 35-wt%E-DC cathode.

Table 4. Resistances in single cells using DC cathode and X-wt%E-DC cathodes

Cathode	Charge transfer resistance (Ωcm²)	Mass transfer resistance (Ωcm²)
DC cathode	0.56	0.93
25-wt%E-DC cathode	0.24	0.93
35-wt%E-DC cathode	0.21	0.70

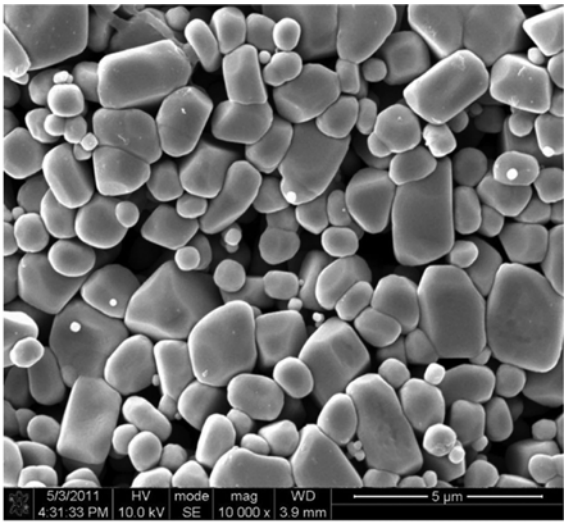

(a)

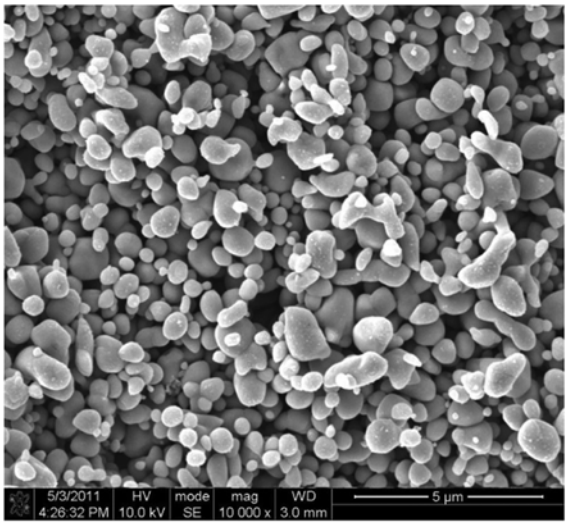

(b)

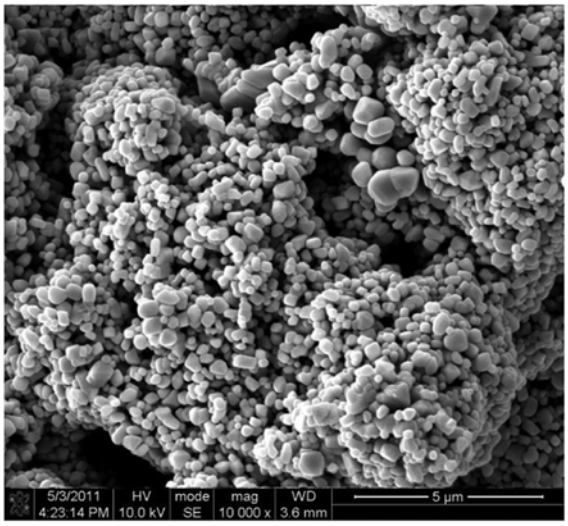

(c)

Fig. 11. SEM images of DC cathode and X-wt%E-DC cathodes after cell operation: (a) DC cathode, (b) 25-wt%E-DC cathode, and (c) 35-wt%E-DC cathode.

case of the MCFC single cells. It is generally known that the width of the first arc in a high-frequency region represents the charge-transfer resistance, the width of the second arc in a low-frequency region shows the mass-transfer resistance, and the intercept on the x-axis indicates the ohmic resistance [22]. The charge transfer resistance and the mass transfer resistance can be separated from the Nyquist plots and are summarized in Table 4. As shown in this table, the charge transfer resistance decreased dramatically after the electrolyte impregnation, and the mass transfer resistance was similar (in the case of the 25-wt%E-DC cathode) or decreased (in the case of the 35-wt%E-DC cathode). A significant decrease in the charge transfer resistance in the X-wt%E-DC cathodes after the electrolyte impregnation could be explained on the basis of the increase in the surface area of the cathode after the electrolyte impregnation. That is, the increase in the three-phase boundary (TPB), in which the cathode reaction occurred, could be attributed to the increase in the surface area of the X-wt%E-DC cathodes after the electrolyte impregnation improved the charge transfer resistance and enhanced the cell performance.

Fig. 11 shows the SEM images of the DC cathode, 25-wt%E-DC cathode, and 35-wt%-DC cathode after the cell operation. From a comparison of Figs. 2(b) and 11(a), we inferred that the Ni branch structure of the DC cathode before the cell operation changed the morphology of the separated NiO particles after the cell operation. This was then considered to be the reason for the increase in the surface area of the DC cathode after the cell operation. As shown in Fig. 11, the NiO particle size decreased with an increase in the amount of the impregnated electrolyte. The increase in the contact area between the Ni and the electrolyte particles inhibited the growth of the NiO particles. This is the reason for the observed large surface area of the electrolyte-impregnated cathode after the cell operation. The high performance and low IR and charge transfer resistance could be realized by this increase in the surface area after the electrolyte impregnation.

We investigated the Li contents of the lithiated NiO cathode in samples of the DC cathode, 25-wt%E-DC cathode, and 35-wt%E-DC cathode after the cell operation via inductively coupled plasma-atomic emission spectrometry (ICP-AES) and have summarized the results in Table 5. The Li contents of the DC cathode, 25-wt%E-DC cathode, and 35-wt%E-DC cathode after the cell operation were 2.1, 2.5, and 2.4 mol%, respectively. It is generally known that the in-situ lithiation into NiO during the cell operation results in lithium contents of 2-3 mol% [23]. This agreed very well with our results. As shown in Table 5, the Li content increased slightly after the electrolyte impregnation. A further lithiation into NiO after the electrolyte impregnation was expected to enhance the electrical conductivities of the 25-wt%E-DC cathode and 35-wt%E-DC cathode. It is generally known that the lithiation into NiO that leads to an increase in the electrical conductivity of lithiated NiO, enables the

Table 5. Lithium contents in DC cathode and X-wt%E-DC cathode after cell operation

Cathode	Lithium contents (mol%)
DC cathode	2.1
25-wt%E-DC cathode	2.5
35-wt%E-DC cathode	2.4

use of in-situ lithiated NiO as an MCFC cathode despite the fact that NiO has poor electrical conductivity [4]. According to van Houten's results [24], the electrical conductivity increased with an increase in the lithium content in lithiated NiO. In particular, the electrical conductivity of lithiated NiO increased rapidly in the range of 0-4 mol% of Li content. This implied that the further lithiation of NiO in the samples of electrolyte impregnation took place during cell operation because of the increase in the contact area between the electrolyte and the Ni particles after the electrolyte impregnation. This increase in the electrical conductivity after the electrolyte impregnation led to an improvement in the cell performance and a decrease in the charge transfer resistance.

CONCLUSION

The MCFC cathode was fabricated successfully by using a simple dry casting method. The as-prepared cathode had the same basic characteristics as those of the conventional cathode fabricated by using the tape casting method and exhibited similar operation results in the single cell. Therefore, the proposed dry casting method is very attractive as a manufacturing method of MCFC electrodes because it is a simplified eco-friendly process.

The electrolyte-impregnated cathodes were also successfully fabricated by using the proposed dry casting method. The high cell performance and the stable cell operation were obtained in a single cell using the 25-wt% electrolyte-impregnated cathode. The improvement in the cell performance in this single cell was attributed to the decrease in the IR and the charge transfer resistance. The decrease in the IR and the charge transfer resistance was caused by the increase in the contact area between the Ni and the electrolyte particles after the electrolyte impregnation enlarged the TPB area in which the cathode reaction occurred. Further, the lithiation into NiO improved the electrical conductivity of the in-situ lithiated NiO cathode. However, a degradation of the cell performance and a decrease in the cell operation time were observed in the single cell using the 35-wt% electrolyte-impregnated cathode because of the rapid increase in the N_2 crossover caused by the poor formation of a wet seal. Hence, the optimum amount of the electrolyte to be impregnated into the cathode that would lead to a high cell performance and long-term stability was determined.

ACKNOWLEDGEMENT

This work was supported by the New & Renewable Energy of the Korea Institute of Energy Technology Evaluation and Planning (KETEP) grant funded by the Korean Government's Ministry of Knowledge Economy (Project No. 2007NFC12P0130502009 & 2008NFC12J0431102010).

REFERENCES

1. S. A. Song, J. Han, S. P. Yoon, S. W. Nam, I.-H. Oh and D. K. Choi, *J. Electrochem. Sci. Technol.*, **1**, 102 (2010).
2. J.-H. Lim, G. B. Yi, K. H. Suh, J.-K. Lee, Y. S. Kim and H.-S. Chun, *Korean J. Chem. Eng.*, **16**, 856 (1999).
3. Y.-S. Kim, H.-S. Choo, M.-C. Shin, M.-Z. Hong, J.-H. Lim and H.-S. Chun, *Korean J. Chem. Eng.*, **17**, 497 (1999).
4. A. Dicks, *Curr. Opin. Solid State Mater. Sci.*, **8**, 379 (2004).
5. Z. P. Liu, P. Y. Guo and C. L. Zeng, *J. Power Sources*, **166**, 348 (2007).
6. E. Park, M. Hong, H. Lee, M. Kim and K. Kim, *J. Power Sources*, **143**, 84 (2005).
7. S. Y. Lee, H.-C. Lim and G.-Y. Chung, *Korean J. Chem. Eng.*, **27**, 487 (2010).
8. S. Randstrom, C. Lagergren and S. Scaccia, *Fuel Cells*, **7**, 218 (2007).
9. B. H. Ryu, I. G. Jang, K. H. Moon, J. Han and T.-H. Lim, *J. Fuel Cell Sci. Technol.*, **3**, 389 (2006).
10. H.-H. Park, C.-I. Jang, H.-S. Shin and K.-T. Lee, *Korean J. Chem. Eng.*, **13**, 35 (1996).
11. X.-J. Luo, B.-L. Zhang, W.-L. Li and H.-R. Zhung, *Ceram. Int.*, **30**, 2099 (2004).
12. F. Li, C. Wang and K. Hu, *Mater. Res. Bull.*, **37**, 1907 (2002).
13. D. Hotza and P. Greil, *Mater. Sci. Eng.*, **A202**, 206 (1995).
14. C. Fu, S. H. Chan, Q. Liu, X. Ge and G. Pasciak, *Int. J. Hydrog. Energy*, **35**, 301 (2010).
15. Z. Lv, T. Zhang, D. Jiang, J. Zhang and Q. Lin, *Ceram. Int.*, **35**, 1889 (2009).
16. Y.-P. Zeng, A. Zimmermann, L. Zhou and F. Aldinger, *J. Eur. Ceram. Soc.*, **24**, 253 (2004).
17. B. H. Ryu, Y. S. Kim, C.-S. Jun and M. Y. Shin, US Patent, 160,181 (2008).
18. G. Xu and C. Yuh, US Patent, 257,721 (2006).
19. B. H. Ryu, Y. S. Kim, C.-S. Jun and M. Y. Shin, US Patent, 157,419 (2008).
20. A. Wijayasinghe, B. Bergman and C. Lagergren, *Solid State Ionics*, **177**, 175 (2006).
21. S. Mitsushima, K. Matsuzawa, N. Kamiya and K. Ota, *Electrochim. Acta*, **47**, 3823 (2002).
22. S. A. Song, M. G. Kang, J. Han, S. P. Yoon, S. W. Nam, I.-H. Oh and D. K. Choi, *J. Electrochem. Soc.*, **158**, B660 (2011).
23. P. A. Lessing, G. R. Miller and H. Yamada, *J. Electrochem. Soc.*, **133**, 1537 (1986).
24. S. van Houten, *J. Phys. Chem. Solids*, **17**, 7 (1960).